ISSN 1995-0780, Nanotechnologies in Russia, 2020, Vol. 15, Nos. 3–6, pp. 370–378. © Pleiades Publishing, Ltd., 2020.
Russian Text © The Author(s), 2020, published in Rossiiskie Nanotekhnologii, 2020, Vol. 15, No. 3, pp. 384–392.

DEVICES AND PRODUCTS BASED ON NANOMATERIALS AND NANOTECHNOLOGIES

Russian Technologies and Nanostructural Materials in High Specific Power Systems Based on Hydrogen–Air Fuel Cells with an Open Cathode

S. I. Nefedkin[a,*], V. E. Guterman[b], A. A. Alekseenko[b], S. V. Belenov[b], A. V. Ivanenko[a], M. A. Klimova[a], V. I. Pavlov[a], S. V. Panov[a], K. O. Paperzh[b], and S. V. Shubenkov[a]

[a] *BMPower company (participant of the Skolkovo project), Moscow, Russia*

[b] *Prometheus R&D LLC (participant of the Skolkovo project), Rostov-on-Don, Russia*

**e-mail: nefedkin@bmpower.ru*

Received June 5, 2020; revised August 10, 2020; accepted August 13, 2020

Abstract—The development of energy systems based on high specific power hydrogen–air fuel cells using domestic nanostructured materials and technologies is an urgent task. The technologies used for manufacturing proton-exchange membrane fuel cells (PEM FC) by the Russian company BMPower using Pt/C-electrocatalysts of the PM series produced by another Russian company, Prometheus R&D, are presented. It has been shown that, in terms of their functional characteristics, catalysts of the PM series are superior to imported analogues. The use of the PM40 catalyst, as well as other innovative solutions in the field of nanotechnology (nanostructured coatings of bipolar plates, formation of an ionomer on the catalytic layer) makes it possible to achieve a specific power of more than 1 kW/kg in the PEM FC power module with air cooling.

DOI: 10.1134/S199507802003009X

INTRODUCTION

Over the last decade, power plants based on hydrogen-air proton-exchange membrane fuel cells (PEM FC) have dominated other types of FC and are actively entering the market of energy sources for autonomous devices and vehicles [1]. Such power plants in the nominal load mode have an efficiency of about 50%, but at partial load it can reach 70% or more. The air-cooled power module makes it possible to develop a specific power in real operating conditions of an unmanned aerial vehicle (UAV) over 1 kW/kg, while the specific energy per unit mass of the power system on board the UAV can reach 700 W h/kg. This is 4–5 times higher than that of lithium-ion batteries (with a high current output) on board of the same UAVs. In real conditions, the energy consumption of lithium-ion batteries, taking into account their incomplete discharge and heat losses at high currents, is only 140–160 W h/kg. Therefore, the use of an energy system based on the PEM FC makes it possible to increase the UAV's flight range by 3–5 times, which corresponds in range to UAVs equipped with internal combustion engines (ICE). However, unlike internal combustion engines, power systems based on proton-exchange membrane fuel cells show a higher efficiency, do not have harmful emissions, show low levels of noise and vibration, which is important for ensuring the stealth of the UAV flight and for better photo and aerial survey [2–6]. High specific characteristics have been achieved by increasing the specific power of the power module itself, reducing the mass of power system components. It does not use massive bipolar plates, humidifiers, heaters, radiators and other elements that are usually used in automotive power plants based on the PEM FC with a closed cathode and liquid cooling. In this paper, a simplified scheme of the power system is implemented, in which hydrogen is supplied from a high-pressure cylinder through a reducer to the anode cavity of the FC, and a supercharger pumps air through corrugated bipolar plates to the cathodes. Thus, the heat released during the operation of the PEM FC is removed, oxygen is supplied, and reaction water is removed with humidified air [2–6].

High specific power of a single FC is achieved by:

—an innovative technology for the formation of polymer electrolyte and catalytic layers, which provides high proton conductivity, self-humidification of the electrolyte and catalytic layers only with reaction water;

—high activity of the catalytic layer. This parameter is primarily determined by the activity of the PM40 catalyst;

—the use of light bipolar plates with a low-resistance corrosion-proof coating for efficient electrical switching of FCs in the power module.

In this paper, along with solving the problem of developing the power system of PEM FC, a successful solution to one of the most difficult problems is presented – the manufacture of highly active nanostructured electrocatalysts, which are not inferior or are even superior to well-known foreign examples. Taking into account the presence of know-how used in the synthesis of catalysts, the emphasis in the work is made on their characterization using modern research and analysis methods, as well as on the results of tests in electrochemical cells and real power systems of the PEM FC with direct air supply.

EXPERIMENTAL

Nanostructured Pt/C-electrocatalysts of the PM series were obtained by liquid-phase synthesis methods according to the original technology of Prometheus R&D, which is in the know-how mode. As a carbon support in the preparation of catalysts containing 20–40 wt % Pt, carbon black Vulcan XC72 (Cabot Co.) was used, for the catalyst with a platinum load of 60 wt % – KetjenblackEC 300J.

The mass fraction of platinum in the samples was determined by gravimetry from the mass of the residue that was not burnt when heated to 800°C. It was taken into account that the carbon support itself burns out without residue.

Powder diffractograms of metal-carbon materials were recorded on an ARL X'TRA automatic diffractometer using CuK_α radiation ($\langle\lambda\rangle$ = 1.5418 Å). The measurements were carried out at room temperature. The samples were thoroughly mixed and placed in a cell 1.5 mm deep or on a backgroundless substrate. Filming was carried out in the range of angles 15–55° with a step of 0.02° and a speed of 8 to 0.5°/min, depending on the task set. The average crystallite size of the metal phase was calculated using the Scherrer equation for the most intense peak (111), as described in [7].

The analysis of the catalyst structure by transmission electron microscopy (TEM) was carried out using a JEM-2100 microscope (JEOL, Japan) operating at an accelerating voltage of 200 kV. To prepare the samples for the study, the electrocatalyst powder (0.5 mg) was placed in 1 mL heptane and dispersed by ultrasound to obtain a homogeneous suspension, one drop of which was deposited on a carbon-coated copper spray grating.

A three-electrode electrochemical cell was used to study the electrochemical behavior of the catalysts. For the working electrode, the end face of a Teflon-reinforced glass-graphite cylinder coated with a thin Pt/C layer was used. For auxiliary electrode, Pt-wire was used, and for the reference electrode, an Ag/AgCl/KCl-electrode was used. For the working electrolyte, a 0.1 M $HClO_4$ solution saturated with argon (when measuring cyclic voltammograms (CV)) or oxygen (when determining the activity of catalysts in the oxygen reduction reaction (ORR)) was applied. All potential values in this work are given relative to a reversible hydrogen electrode (RHE).

The electrochemical surface area (ESA) of platinum was determined by the CV method on a stationary electrode. A suspension (catalytic ink) of the studied Pt/C materials was used to prepare the working electrode. To prepare the ink, a 6 mg sample of the catalyst was placed in a mixture of 900 μL isopropanol and 100 μL an aqueous emulsion of the Nafion® 0.5% polymer. Then the suspension was stirred on a mechanical magnetic stirrer and subjected to dispersion in an ultrasonic bath. An aliquot of ink with a volume of 6 μL was applied to the glass graphite end face of a polished and degreased rotating disk electrode (RDE) with an area of 0.196 cm^2, controlling the weight of the drop. Initially, for surface standardization, 100 cyclic voltammograms were recorded in the potential range of 0.04–1.2 V at a potential sweep rate of 200 mV/s. Then, two cyclic voltammograms were recorded at a potential sweep rate of 20 mV/s. The electrochemical surface area was calculated from the half-sum of the amounts of electricity consumed for the electrochemical desorption and adsorption of hydrogen using the voltammogram of the second cycle, as described in [8].

The activity of the catalyst in the ORR was determined by voltammetry on a rotating disk electrode in the potential range from 0.04 to 1.2 V. The electrolyte (0.1 M $HClO_4$) was saturated with oxygen for 60 min, after which voltammograms were measured at potential sweep towards higher values at a rate of 20 mV/s at various speeds of rotation (400, 900, 1600, and 2500 rpm) of the disk electrode. To take into account the contribution of the ohmic potential drop and processes not associated with the ORR, the voltammograms obtained during the potential sweep towards more positive values were normalized according to generally accepted techniques [9, 10]. For this, the potential of the electrode under study was refined according to the formula $E = E_{meas} - I_tR$, where E_{meas} is the set value of the potential, I_tR is the ohmic potential drop, equal to the product of the current strength and the resistance of the R-layer of the solution between the reference electrode and the test electrode, which was in this case 23 ohms. This resistance value is consistent with the data in [10]. The contribution of the processes occurring at the electrode in the deoxygenated solution (Ar atmosphere) was taken into account by subtracting from the voltammogram a similar curve recorded during measurements in an Ar atmosphere: ($I(O_2) - I(Ar)$), as described in [11]. The catalytic activity of catalysts in the ORR (kinetic current) was determined from normalized voltammograms taking into account the contribution of mass transfer under the conditions of RDE [11]. The kinetic

Table 1. Structural characteristics of Pt/C-electrocatalysts

Sample	Mass fraction of Pt in catalysts, ω(Pt), %	Average size of Pt crystallites, D_{av}, nm (XRD)	Average size of platinum nanoparticles, D_{av}, nm (TEM)
PM20	20	2.2	3.1
PM30	30	2.9	2.9
PM40	40	2.1	3.1
PM60	60	4.0	3.9
HiSPEC 3000	20	2.3	2.0–2.5 [14, 15]
E-TEK 40	40	3.7	3.2–3.7 [16, 17]

Table 2. Parameters characterizing the electrochemical behavior of Pt/C electrocatalysts

Sample	ESA, $m^2/g(Pt)$	I_k, A at 0.90 V	I_k, A/g(Pt) at 0.90 V	$E_{1/2}$, V	Relative stability, % (5000 cycles, 0.6–1.0 V)
PM20	120	1.9	250	0.92	86
PM30	98	2.1	208	0.92	86
PM40	88	2.5	186	0.94	86
HiSPEC3000	84	1.3	182	0.91	82
E-TEK 40	42	1.4	134	0.89	

current was calculated using the Koutecky–Levich equation:

$$1/j = 1/j_k + 1/j_d,$$

where j is the experimentally measured current, j_d is the diffusion current, j_k is the kinetic current. The kinetic currents were calculated for a potential of 0.90 V (RHE).

To assess the stability of electrocatalysts, the CV method (5000 cycles) was used in the potential range of 0.6–1.0 V with a potential sweep rate of 100 mV/s. This technique makes it possible to diagnose differences in the stability of platinum-containing catalysts, which is confirmed, for example, by the results of papers [8, 12]. Cycling was carried out in an argon atmosphere. After every 500 cycles, two cyclic voltammograms were recorded at a potential sweep rate of 20 mV/s in the potential range of 0.04–1.2 V, from the hydrogen region of which the ESA was calculated. The degradation of the material was assessed not only by the change in ESA, as was carried out in [8, 12], but also by comparing the values of kinetic currents in the ORR before and after the stress test.

Electrocatalysts were tested in a membrane electrode assembly (MEA) of a hydrogen-air FC as follows. By dispersing the electrocatalyst and

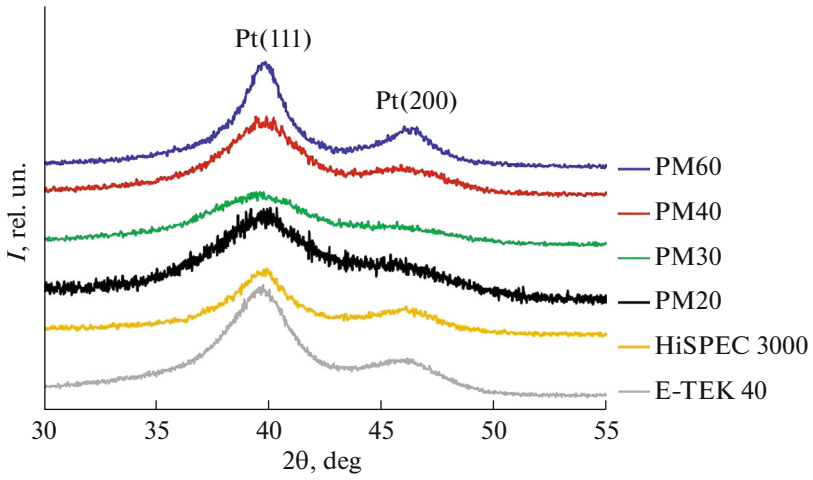

Fig. 1. (Color online) X-ray diffraction patterns of Pt/C-electrocatalysts of the PM series and imported analogs.

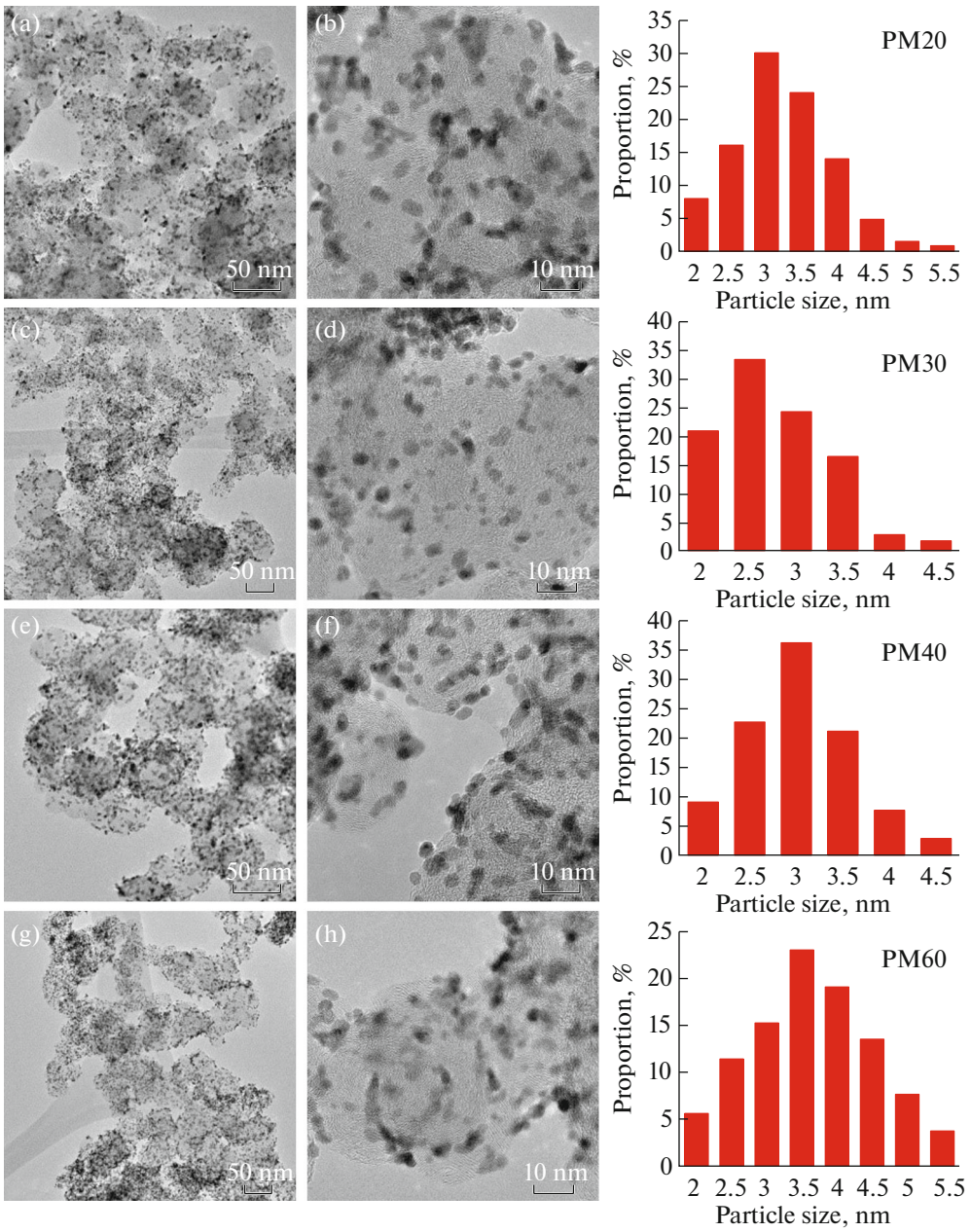

Fig. 2. (Color online) TEM images of Pt/C materials and histograms of nanoparticle size distribution: (a, b) PM20, (c, d) PM30, (e, f) PM40, (g, h) PM60.

Nafion emulsion (DE-1021, 10 wt %) (mass ratio Nafion/Carbon = 0.7) in a water/isopropanol mixture, catalytic ink was prepared, which was then applied to a Freudenberg gas diffusion layer. To form the cathode and anode layers, the studied catalyst was applied in an amount necessary to achieve a platinum loading of 0.4 mg/cm^2. The MEA was assembled in air. The pressing was carried out for three minutes at $T = 130°$ C and $P = 80$ atm/cm^2. The MEA was tested in an Electrochem cell with an active area of 1 cm^2 at the GreenLight Innovation G40 station (hydrogen/air, hydrogen flow rate 0.1 l/min, air – 0.4 l/min, gas humidification 100%, $T = 20°$C). An Elins P40X potentiostat was used to record cyclic voltammograms; the recording time for one voltammogram was 13 min. The activity of Pt/C samples of the PM series (Prometheus R&D) was compared with the parameters of commercial Pt/C electrocatalysts HiSPEC3000 (Johnson Matthey, 20 wt % Pt) and E-TEK 40 (E-tek, 40 wt % Pt).

To test the developed catalyst in the power module, it was applied to the surface of the microporous layer of a Freudenberg H24C3 gas-diffusion electrode. For application, the method of layer-by-layer ultrasonic

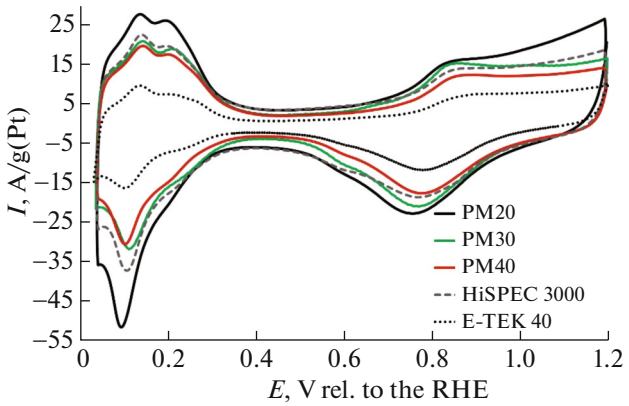

Fig. 3. (Color online) Cyclic voltammograms of Pt/C catalysts. Second cycle. The potential sweep rate is 20 mV/s, and the electrolyte is a 0.1 M $HClO_4$ solution saturated with argon.

spraying of catalytic ink containing a catalyst was used, as well as a one-stage silk-screen printing process from a catalytic paste. After applying the catalysts to the gas diffusion layer, a fuel cell with an active surface of 54 cm^2 was formed by hot pressing. The power module PEM FC for testing the catalysts consisted of 96 fuel cells, which were switched through BMPower bipolar cells based on corrugated titanium foil with a protective coating and were pulled together with end plates using pins. The air was supplied by a blower installed at the battery outlet (air extraction). The current-voltage and resource characteristics of the energy module were determined on a specialized stand with a controlled supply of 99.995% purity hydrogen with an overpressure of 0.4–0.5 bar. Electrical control and measurements were performed using an ACTACOM EA-EL 9200-420 B electronic load.

RESULTS AND DISCUSSION

Nanostructured catalysts PM20, PM30, PM40, and PM60 containing from 20 to 60 wt % Pt (Table 1) are platinum nanoparticles, distributed properly on the surface and in the pores of the particles of carbon supports.

According to the results of X-ray diffractometry, the electrocatalysts of the PM series are characterized by an average platinum crystallite size from 2.1 to 4.0 nm, the commercial analogs studied, about 2 nm (HiSPEC3000) and 4 nm (E-TEK 40) (Table 2). The

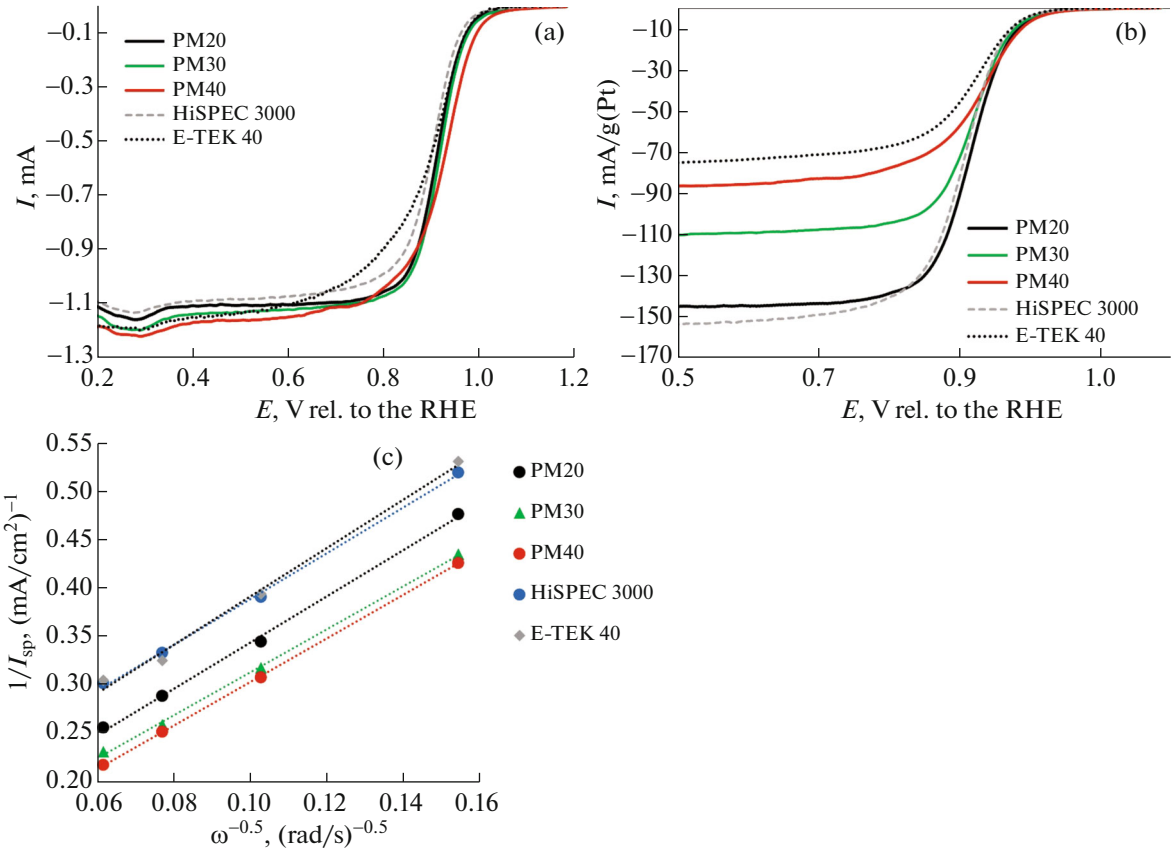

Fig. 4. (Color online) Voltammograms of oxygen electroreduction on different electrocatalysts at a rotation speed of 1600 rpm (a, b) and the dependence of the current strength on the rotation speed of the disk electrode in the Koutecky–Levich coordinates (c). The potential sweep rate is 20 mV/s, and the electrolyte is a 0.1 M $HClO_4$ solution saturated with oxygen.

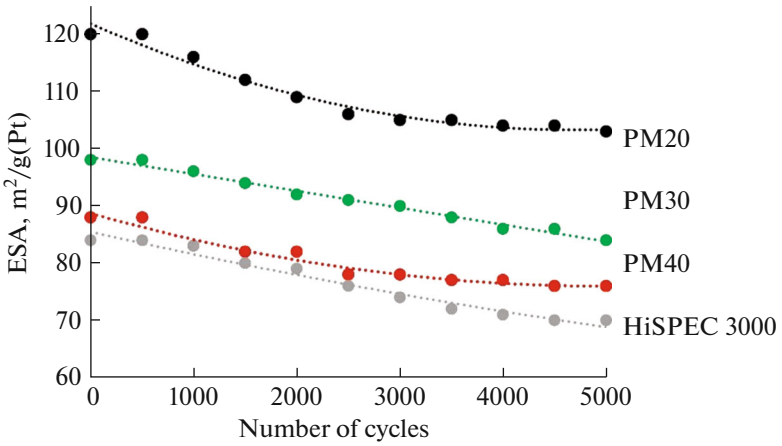

Fig. 5. (Color online) Change in the area of the electrochemical surface area of Pt during stress testing of catalysts (5000 cycles in the range of 0.6–1.0 V).

largest crystallite size, about 4.0 nm, is characteristic of materials with the highest platinum loading PM60 (60 wt % Pt) and E-TEC 40 (40 wt % Pt), the X-ray diffraction patterns of which show a high and relatively narrow in comparison with other materials maximum of 111 platinum with a 2θ angle of about 40 degrees (Fig. 1).

The values of the average sizes of nanoparticles determined from TEM images are generally consistent with the results of calculating the size of crystallites using the Scherrer equation (Table 1). All samples of the PM series are characterized by a uniform distribution of platinum nanoparticles over the surface of the carbon carrier (Fig. 2). The photographs of all the samples show the presence of a small number of aggregates about 4–5.5 nm in size (Fig. 2).

An increase in the content of platinum in catalysts, as a rule, leads to a decrease in the average distance between nanoparticles, which increases the probability of their coalescence and, as a consequence, causes an increase in the average particle size [13]. Among the electrocatalysts under study, the largest nanoparticles and, as noted, platinum crystallites are characterized by samples with a high metal loading: PM60 (60 wt % Pt) and E-TEC 40 (40 wt % Pt) (Fig. 2, Table 1).

Typical cyclic voltammograms of the studied samples are shown in Fig. 3. In almost the entire potential range, the currents on the cathodic and anodic branches of cyclic voltammograms per unit mass of platinum increase in series: E-TEK 40 ≪ PM40 < PM30 ≈ HiSPEC 3000 < PM20. Catalysts of the PM series show higher ESA values than imported analogues with the same platinum content (Table 2).

Judging by the results of X-ray phase analysis (XRD) and TEM shown in Figs. 1, 2 and in Table 1, high ESA values are due not so much to the small size of platinum nanoparticles, but to the uniformity of their spatial distribution (weak aggregation of particles) and high availability with respect to the electrolyte and reagent.

Apparently, the positive features of the structure of catalysts of the PM series are due to the use of colloidal chemistry methods in the technology of their synthesis, developed at Prometheus R&D.

Catalytic activity of Pt/C catalysts[1] was determined by the method of voltammetry on the RDE, registering a series of curves at electrode rotation speeds of 400, 900, 1600, and 2500 rpm. These curves (Figs. 4a, 4b) were used to analyze the dependence of the current at a potential of 0.90 V on the rotational speed of the disk electrode in the Koutecky–Levich coordinates (Fig. 4c). This made it possible to determine the values of the kinetic parameters of the ORR and to compare the activities of the studied catalysts (Table 2).

According to the increase in the mass activity in the ORR and the potential of the RVC half-wave, the studied catalysts are respectively arranged in series: E-TEK 40 ≪ HiSPEC 3000 ≈ PM40 < PM30 < PM20 and E-TEK 40 < HiSPEC 3000 < PM30 = PM20 < PM40 (Table 2). Thus, the activity of catalysts of the PM series in the ORR exceeds the activity of foreign analogues.

Stress testing of Pt/C catalysts (5000 cycles in the potential range of 0.6–1.0 V) showed their high stability (Fig. 5, Table 2). It is important that the relative stability of catalysts of the PM20–PM40 series does not depend on the metal content in them and slightly

[1] Electrocatalyst with a high loading of PM60 platinum requires the selection of an optimal composition of catalytic ink and a different Nafion/carbon carrier ratio than PM20–PM40 [18]. The electrochemical behavior of this catalyst has not been studied.

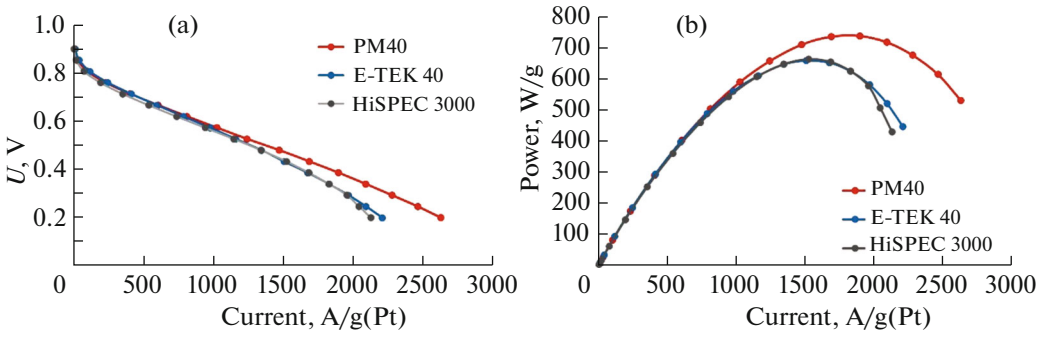

Fig. 6. (Color online) Current-voltage (a) and power (b) specific characteristics of the MEA with catalysts PM40, HiSPEC 3000, and E-TEK 40.

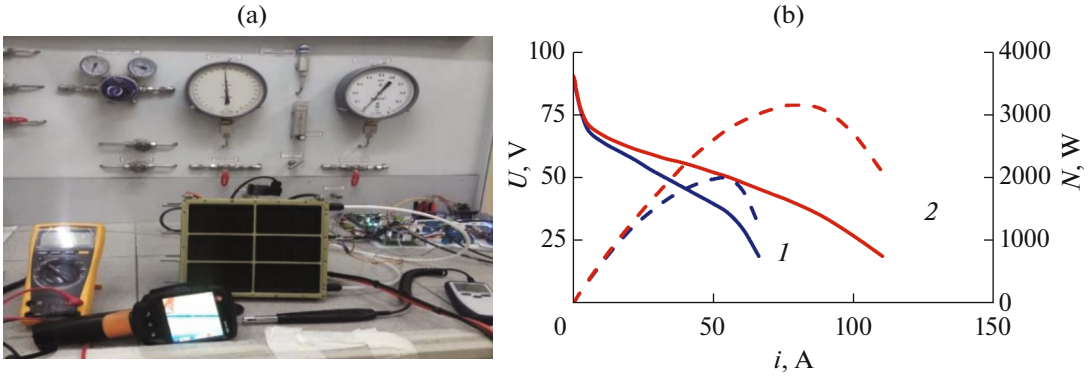

Fig. 7. (Color online) Tests of a power module of 96 fuel cells (BMPower) with an open cathode without external humidification of the reaction gases; $T = 23°$ C, $RH = 60\%$; (*1*) membrane (30 μm), (*2*) DMD technology. P40 catalyst by Prometheus R&D. m_s^{Pt} (mg/cm^2): anode—0.2, cathode—0.4. Bipolar titanium elements with coating by BMPower (a); current-voltage and power characteristics of the power module (b).

exceeds the stability of foreign analogues.[2] The high values of the initial ESA, mass activity, and stability of PM catalysts confirmed the promising nature of their use in the design of the MEA for hydrogen-air fuel cells.

It is known that the efficiency of using platinum-containing catalysts in the MEA of proton-exchange membrane fuel cells does not always correlate with their behavior in an electrochemical cell, since the operating conditions of the catalyst in the MEA differ significantly from those for a half-cell with a liquid electrolyte [19–21]. In particular, in the catalytic layer of the MEA, the conditions for supplying reagents and removing products to/from platinum nanoparticles change significantly; an important role is played by the moisture content of the supplied gases, the rate of their supply, the features of the distribution of the proton-conducting ionomer in the catalytic layer, etc. From the point of view of optimizing the mass fraction of platinum in the electrocatalyst, the composition and thickness of the catalytic layer, electrocatalysts with a 40% platinum loading with a precious metal content of 0.2–0.4 mg/cm^2 of the membrane geometric surface are most widely used in the design of the MEA [21]. Taking the above into account, the PM40 sample was selected from catalysts of the PM series for testing in the MEA. At the same time, imported catalysts, previously studied in half-cells, were used as reference samples—HiSPEC3000, which showed a relatively high activity, and E-TEK 40, containing, like PM40, 40 wt % Pt.

The results of comparative tests of the catalysts PM40, E-TEK 40, and HiSPEC 3000 at the MEA confirmed the highest efficiency of PM40 (Fig. 6). Thus, the maximum specific power obtained in the MEA using the PM40 catalyst was 736 W/g(Pt) or 341 mW/cm^2, which exceeds the power values for E-TEC 40 and HiSPEC3000 (657 and 662 W/g(Pt), respectively)). Note that the values of the maximum specific power of the MEA obtained using imported materials are in good agreement with the results [21].

When using the PM40 catalyst for the MEA at $T =$ 20°C and 100% humidity of gases, an increase in its

[2] Due to the low values of mass activity (Table 2), stress testing of the E-TEK 40 electrocatalyst was not performed.

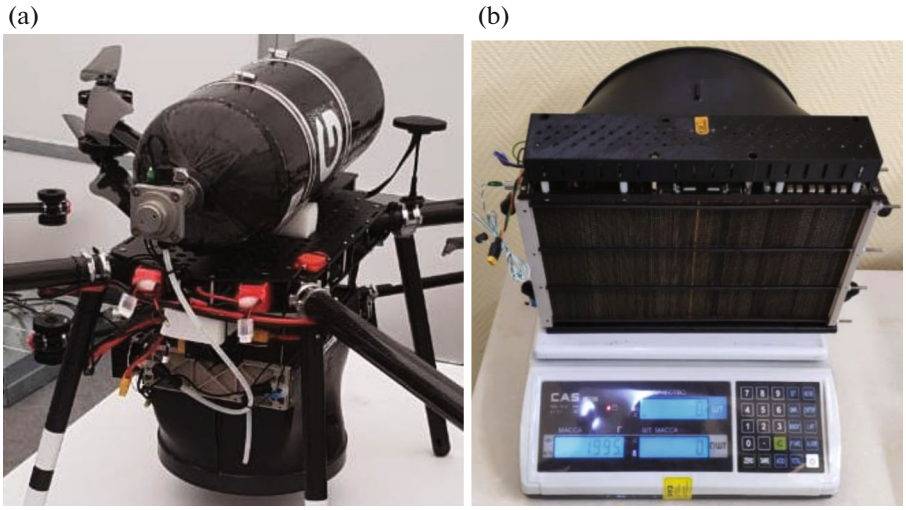

Fig. 8. (Color online) UAV equipped with power system PEM FC by BMPower with direct air supply (a) and power module $N =$ 2 kW by BMPower (b).

functional characteristics by more than 10% compared to imported analogues was recorded. Thus, comparative tests of the catalysts in the MEA confirmed the high activity of the domestic material PM40 and made it possible to proceed to tests in the power module of the PEM FC.

The catalyst deposition method is an important element of the technology that determines not only the characteristics of the MEA, but also its cost. The study showed that when the catalyst is applied to the gas diffusion layer by ultrasonic layer-by-layer spraying of catalytic ink and by silk-screen printing from catalytic paste, their current-voltage characteristics (CVC) in the energy module are practically the same. The technology of forming a membrane on a gas diffusion layer from an ionomer (DMD technology) was also used. As a result, it was confirmed that it is possible to manufacture an MEA based on a simpler and cheaper technology that does not require the use of complex equipment.

The PM40 catalyst was also tested in a power module consisting of 96 fuel cells (Fig. 7). Current-voltage characteristics were measured at room temperature of the incoming air, no special measures were taken to humidify the air.

As seen in Fig. 6b, when the Nafion 211 membrane is used in the MEA, a flat current-voltage characteristic is achieved under these conditions, which noticeably improves upon switching to the DMD technology. Based on the results of the tests carried out, the developed catalyst was recommended for use in power systems for UAVs, which are manufactured by BMPower (Skolkovo). Figure 8 shows one of such power systems with a specific power of EM of 1 kW/kg and a specific system energy of 700 W h/kg (when used in the UAV application) and a power module of 2 kW.

CONCLUSIONS

It is shown that domestic fuel cells and power plants based on them are not inferior to the best samples of similar products available to consumers in the world market. The high specific power of the energy module manufactured by BMPower (up to 1 kW/kg) and the power consumption of the PEM FC power system (700 W h/kg) are due to a combination of innovative solutions, the quality of materials and nanotechnologies used in the manufacture of key components of proton-exchange membrane fuel cells. One of these components are nanostructured Pt/C-electrocatalysts produced by Prometheus R&D based on original liquid-phase synthesis techniques. These materials demonstrate functional characteristics that are not inferior or superior to those of analogs produced by foreign companies, leaders in the world catalyst market. Compared to foreign samples, electrocatalysts of the PM series are characterized by a narrow dispersion of the size and spatial distribution of platinum nanoparticles, higher values of ESA, mass activity in the oxygen reduction reaction, and corrosion-morphological stability.

FUNDING

This work was supported by the National Research University MPEI and the Southern Federal University.

REFERENCES

1. Y. Wang, D. F. Ruiz Diaz, K. S. Chen, et al., Mater. Today **32**, 178 (2020).
2. O. Gonzalez-Espasandin, T. J. Leo, and E. Navarro, Sci. World J., 497642 (2014).
3. R. W. Atkinson, M. W. Hazard, J. A. Rodgers, et al., J. Electrochem. Soc. **164**, F46 (2017).

4. A. Datta and W. Johnson, J. Propuls. Power **30**, 490 (2014).
5. Z. F. Pan, L. An, and C. Y. Wen, Appl. Energy **240**, 473 (2019).
6. S. A. Kirakosyan, A. A. Alekseenko, V. E. Guterman, V. A. Volochaev and N. Yu. Tabachkova, Nanotechnol. Russ. **11**, 287 (2016).
7. A. A. Alekseenko, V. E. Guterman, S. V. Belenov, et al., Int. J. Hydrogen Energy **43**, 3676 (2018).
8. K. Shinozaki, J. W. Zack, S. Pylypenko, et al., J. Electrochem. Soc. **162**, F1384 (2015).
9. D. Van der Vliet, D. S. Strmcnik, C. Wang, et al., J. Electroanal. Chem. **647**, 29 (2010).
10. W. J. Khudhayer, N. N. Kariuki, X. Wang, et al., J. Electrochem. Soc. **158**, 1029 (2011).
11. A. A. Alekseenko, E. A. Moguchikh, O. I. Safronenko, and V. E. Guterman, Int. J. Hydrogen Energy **43**, 22885 (2018).
12. Zh. Xua, H. Zhang, H. Zhong, et al., Appl. Catal. B **111–112,** 264 (2012).
13. O.-H. Kim, C.-Y. Ahn, S. Y. Kang, et al., Fuel Cells **19**, 695 (2019).
14. Z. Li, X. Deng, H. Zhou, et al., J. Solid State Electrochem. **24**, 195 (2020).
15. J. Perez, V. A. Paganin, and E. Antolini, J. Electroanal. Chem. **654**, 108 (2011).
16. F. Godínez-Salomón, E. Arce-Estrada, and M. Hallen-López, Int. J. Electrochem. Sci. **7**, 2566 (2012).
17. Y. Lv, H. Liu, J. Li, et al., J. Electroanal. Chem. **873**, 114444 (2020).
18. S. Martens, L. Asen, G. Ercolano, et al., J. Power Sources **392**, 274 (2018).
19. A. Orfanidi, P. Madkikar, H. A. El-Sayed, et al., J. Electrochem. Soc. **164**, F418 (2017).
20. F. Barbir, *PEM Fuel Cells: Theory and Practice* (Elsevier, New York, 2005).
21. B. Millington, S. Du, and B. G. Pollet, J. Power Sources **196**, 9013 (2011).

Translated by S. Avodkova